Statistically Reliable and Fast Direct Estimation of Phase-Amplitude Cross-Frequency Coupling

Tolga Esat Özkurt*

***Abstract*—There is growing interest in phase-amplitude cross-frequency coupling (PAC), which is widely observed in human and animal brain recordings. The choice of the estimation method is vital while extracting accurate PAC parameters from data. Two desired properties of PAC estimators are reliability and computational efficiency. This study offers a methodology called normalized direct PAC (ndPAC) for the rapid and statistically reliable estimation of PAC strength. A plain confidence limit formula, depending solely on data length and confidence level, is derived. Confidence level derivation is validated numerically. It is shown through simulations that ndPAC exhibits high specificity and sensitivity performances. The suggested methodology is also demonstrated on monkey electrocorticogram recorded during a visual task.**

***Index Terms*—Confidence level, electrocorticogram (ECoG), neuronal oscillations, phase-amplitude coupling (PAC).**

I. Introduction

A CONSIDERABLE part of neural information is known to be encoded temporally [1], [2]. Phase-amplitude coupling (PAC) is an interesting temporal phenomenon that was shown to exist commonly in human and animal brain recordings. PAC refers to the interaction between the amplitude of a high-frequency component and the phase of a low-frequency component in electrophysiological signals [3]–[5]. It might indicate a control of low-frequency oscillations over the activity of microcellular level neuronal assemblies associated with high-frequency oscillations.

Modulation of PAC is also of great interest, as it yields information regarding either task state [6]–[9] or medical state [10], [11]. This modulation can be observed by means of four PAC parameters: 1) strength, 2) phase frequency, 3) amplitude frequency, and 4) spatial topography. The mapping between brain state and PAC can be described as variations in one single parameter or combinations of these parameters.

Correspondence of all these PAC parameters to different brain states has been presented in recent literature. Händel and Haarmeier [6] showed an association between PAC strength and visual discrimination capability. Importantly, the coupling strength was not induced by oscillation powers at one of the coupling frequencies, which implied the exclusive role of PAC strength over the visual task performance. Axmacher *et al.* [9] reported the modulation of PAC strength with the working memory load. When the memory load was increased, the phase frequency shifted to lower frequencies implying necessary increase of cycle length to cover large number of representations of memory. Similar to the case in [6], changes in power at the coupling frequencies were correlative neither to the PAC strength nor to the memory load. Another study by Özkurt *et al.* [11] demonstrated that not only does the PAC strength in the subthalamic nucleus decrease but also the coupling amplitude frequency shifts to higher frequency ranges upon dopaminergic administration. Using subdural electrodes in epileptic patients, Voytek *et al.* [8] showed that gamma amplitude was coupled to both alpha and theta phase for various tasks. However, only visual tasks favored the influence of alpha/ gamma PAC significantly over the occipital regions.

In this study, we consider rapid assessment of statistically reliable estimations for the parameter of PAC strength. In this respect, we derive a basic confidence bound formula depending only on data length and confidence level in order to compute a statistical threshold for PAC estimates. PAC estimation is realized via a "normalized direct PAC method." Thresholding by the derived probabilistic bound increases the specificity of the estimation. Robustness and validity of derivations are demonstrated on simulated data with additive background and unwanted noise. The suggested methodology is also applied on monkey ECoG data acquired during a visual task.

II. Algorithm Development

A. Derivation of Confidence Limit

In this section, a simple formula is derived to compute a confidence limit for direct PAC (dPAC) estimate, which is expressed as [5]

$$\hat{\rho}_D := \frac{1}{\sqrt{N}} \frac{\left| \sum_{n=1}^{N} a_H(n) e^{i\varphi_L(n)} \right|}{\sqrt{\sum_{n=1}^{N} a_H(n)^2}}. \quad (1)$$

Here, $a_H(n)$ is the random amplitude vector and $\varphi_L(n)$ is the random phase vector extracted from high- and low-bandpass filtered signals (typically via Hilbert transform) with data length *N*, respectively. The dPAC method aims at quantifying the coupling strength between amplitudes a_H and phases φ_L of a common signal (or two different signals) for a frequency band pair. A coupling portrait is obtained by an estimation of the coupling strength for each pair in a chosen frequency range.

Manuscript received December 1, 2011; revised March 9, 2012; accepted April 6, 2012. Date of publication April 16, 2012; date of current version June 20, 2012. This work was supported by the Scientific and Technological Research Council of Turkey under TÜBİTAK BİDEB 2232 Fellowship Programme. *Asterisk indicates corresponding author.*

The author is with the Department of Health Informatics, Informatics Institute, Middle East Technical University, Ankara 06800, Turkey (e-mail: tolga@ii.metu.edu.tr).

Digital Object Identifier 10.1109/TBME.2012.2194783

For simplicity of notation, we denote $y := a_H$ and $z := e^{i\varphi_L} = \cos\varphi_L + i\sin\varphi_L = x_1 + ix_2$. We assume that the amplitude is normally distributed with zero mean and unit variance, while the phase is uniformly distributed between $-\pi$ and $+\pi$, i.e., $a_H \sim N(0,1)$ and $\varphi_L \sim U(-\pi,\pi)$.

Then, the probability density function (pdf) for *y* is

$$f_Y(y) = \frac{1}{\sqrt{2\pi}} e^{-0.5y^2} \tag{2}$$

and the pdf for $x_1 = \cos\varphi_L$ and $x_2 = \sin\varphi_L$ can be shown to be same with a change of variable [12]

$$f_X(x) = f_{X_1}(x) = f_{X_2}(x) = \frac{1}{\pi}\frac{1}{\sqrt{1-x^2}}, \quad -1 < x < 1. \tag{3}$$

We would like to identify the pdf for

$$\left(\sum_{n=1}^{N} y_n z_n\right)^2 = \left(\sum_{n=1}^{N} y_n x_{1n}\right)^2 + \left(\sum_{n=1}^{N} y_n x_{2n}\right)^2 \tag{4}$$

where both terms of the expression have identical pdf. Even though they are not independent, the maximum expected value would be twice the value we would get from the pdf of $(\sum_{n=1}^{N} y_n x_{1n})^2$ or $(\sum_{n=1}^{N} y_n x_{2n})^2$.

Accordingly, we take the direction to derive confidence for $(\sum_{n=1}^{N} y_n x_n)^2$where $x_n \sim f_X(x)$. Toward this goal, we first search for the pdf of

$$\sum_{n=1}^{N} x_n y_n = \sum_{n=1}^{N} v_n \tag{5}$$

where x_n, y_n and, hence, v_n are assumed to be independent and identically distributed (i.i.d.).

It is well known that pdf of sums of i.i.d. random variables can be found out from the *N*th power of the characteristic function $\Phi_V(\omega)$ [12]

$$\begin{aligned}\Phi_{\sum V_n}(\omega) &:= E\left\{\exp\left(i\omega\sum_{n=1}^{N} v_n\right)\right\} \\ &= E\{e^{i\omega v_1}\}E\{e^{i\omega v_2}\}\ldots E\{e^{i\omega v_N}\} \\ &= [\Phi_V(\omega)]^N.\end{aligned} \tag{6}$$

Our strategy is 1) to find pdf of v_n denoted by $f_V(v)$, 2) obtain its characteristic function by a Fourier-like transform of $f_V(v)$, 3) take the *N*th power and finally 4) find the pdf of (5) via an inverse Fourier transform.

1) The pdf of multiplication of two random variables can be obtained using Rohatgi's formula [13]

$$\begin{aligned}f_V(v) &= \int_{-\infty}^{\infty} f_X(x) g\left(\frac{v}{x}\right)\frac{1}{|x|}dx \\ &= \int_{-1+\varepsilon}^{1+\varepsilon} \frac{1}{\pi}\frac{1}{\sqrt{1-x^2}}\frac{1}{\sqrt{2\pi}} e^{-0.5(v^2/x^2)}\frac{1}{|x|}dx, \quad \varepsilon\to 0\end{aligned} \tag{7}$$

where $g(.) := f_Y(y)$ and $v := xy$. Since the integrand in (7) is even, it can be rewritten as

$$f_V(v) = A\int_{x=\varepsilon}^{1+\varepsilon}\frac{1}{x}\frac{1}{\sqrt{1-x^2}} e^{-0.5(v^2/x^2)}dx \tag{8}$$

where $A := \frac{\sqrt{2}}{\pi^{3/2}}$ is a constant term.

2) The characteristic function for (8) is found via Fourier transform operator *F*

$$\begin{aligned}\Phi_V(\omega) &= F\{f_V(v)\} = \int_{v=-\infty}^{\infty} f_V(v) e^{i\omega v}dv \\ &= A\int_{v=-\infty}^{\infty}\int_{x=\varepsilon}^{1+\varepsilon}\frac{1}{x}\frac{1}{\sqrt{1-x^2}} e^{-0.5(v^2/x^2)} e^{i\omega v}dxdv.\end{aligned} \tag{9}$$

The order of the integration can be rewritten using Fubini's theorem [14]

$$\Phi_V(\omega) = A\int_{x=\varepsilon}^{\varepsilon+1}\frac{1}{x}\frac{1}{\sqrt{1-x^2}}\int_{v=-\infty}^{\infty} e^{-0.5(v^2/x^2)} e^{i\omega v}dvdx. \tag{10}$$

As the Fourier transform of a Gaussian function is also a Gaussian

$$F\left\{e^{-0.5(v^2/x^2)}\right\} = x\sqrt{2\pi}e^{-0.5x^2\omega^2} \tag{11}$$

(9) becomes

$$\Phi_V(\omega) = AC\int_{x=\varepsilon}^{\varepsilon+1}\frac{e^{-0.5\omega^2x^2}}{\sqrt{1-x^2}}\,dx \tag{12}$$

where $C := \sqrt{2\pi}$ is another constant term. With a change of variable $x = \sin\theta$, (12) simplifies to

$$\begin{aligned}\Phi_V(\omega) &= AC\int_{\theta=0}^{0.5\pi}\frac{e^{-0.5\omega^2\sin^2\theta}}{\cos\theta}\cos\theta d\theta \\ &= AC\int_{\theta=0}^{0.5\pi} e^{-m\sin^2\theta}\,d\theta\end{aligned} \tag{13}$$

where $m := 0.5\omega^2$. Using the well-known Maclaurin series of exponential

$$e^{-m\sin^2\theta} = \sum_{n=0}^{\infty}\frac{(-1)^n m^n(\sin\theta)^{2n}}{n!}$$

we reformulate the integral

$$\begin{aligned}\Phi_V(\omega) &= AC\int_{\theta=0}^{0.5\pi}\sum_{n=0}^{\infty}\frac{(-1)^n m^n(\sin\theta)^{2n}}{n!}d\theta \\ &= AC\sum_{n=0}^{\infty}\frac{(-1)^n m^n}{n!}\int_{\theta=0}^{0.5\pi}(\sin\theta)^{2n}d\theta.\end{aligned} \tag{14}$$

This expression can be converted to "beta function" *B* [15]

$$\Phi_V(m) = 0.5AC\sum_{n=0}^{\infty}\frac{(-1)^n m^n}{n!}B\left(\frac{2n+1}{2},\frac{1}{2}\right) \tag{15}$$

which might be written in terms of gamma function Γ

$$\Phi_V(m) \;=\; 0.5AC\sum_{n=0}^{\infty}\frac{(-1)^n m^n}{n!}\frac{\Gamma(n+0.5)\Gamma(0.5)}{\Gamma(n+1)}. \quad (16)$$

Using gamma function properties, (16) simplifies to

$$\Phi_V(m) = 0.5\pi AC\sum_{n=0}^{\infty}\frac{(-1)^n m^n}{n!}\frac{(2n)!}{4^n(n!)^2}$$
$$= \sum_{n=0}^{\infty}\frac{(-1)^n m^n (2n)!}{4^n (n!)^3}. \quad (17)$$

Equation (17) can be further reduced to a confluent hypergeometric function [16]

$$\Phi_V(m) =_1 F_1(0.5,\, 1;\, -m). \quad (18)$$

Utilizing an identity of hypergeometric functions [17]

$${}_1F_1(a, 2a; x) = (0.25x)^{0.5-a}e^{0.5x}\Gamma(a+0.5)I_{a-0.5}(0.5x) \quad (19)$$

where *I*(.) is the modified Bessel function. Equation (18) can be shown to be equivalent to contain multipliers of exponential and zero-ordered modified Bessel functions

$$\Phi_V(m) = e^{-0.5m}I_0(-0.5m). \quad (20)$$

The characteristic function eventually becomes $\Phi_V(\omega) = e^{-0.25\omega^2}I_0(-0.25\omega^2)$.

3) The *N*th power of the characteristic function is simply

$$\left[\Phi_V(\omega)\right]^N \;=\; e^{-0.25N\omega^2}\left[I_0(-0.25\omega^2)\right]^N. \quad (21)$$

Here, we exploit recently presented Baricz's expansion for the powers of modified Bessel function, which is based on an Euler's iterative formula for MacLaurin series [18]

$$\left[I_0(0.25\omega^2)\right]^N = \sum_{k=0}^{\infty}\frac{\zeta_k(N)(0.125\omega^2)^{2k}}{(k!)^2}$$
$$= \sum_{k=0}^{\infty}\zeta'(k,N)\omega^{4k} \quad (22)$$

where $\zeta'(k,N) := \frac{\zeta_k(N)}{(k!)^2 2^{6k}}$ can be computed via an iterative formulation

$$\zeta_k = \frac{1}{k}\sum_{p=1}^{k}[p(N+1)-k](C_k^p)^2\zeta_{k-p} \quad (23)$$

and $\zeta_k = 1$ for any *N* [18].

4) Using the identity for the Fourier transform of a derivative of a function

$$F\left\{g^{(n)}(x)\right\} = (-i\omega)^n G(\omega)$$

we show that the inverse Fourier of (21) is

$$f_{V_N}(x) = \; F^{-1}\left\{\left[\Phi_V(\omega)\right]^N\right\}$$
$$= F^{-1}\left\{\sum_{k=0}^{\infty}\zeta'(k,N)e^{-0.25N\omega^2}\omega^{4k}\right\} \quad (24)$$

$$f_{V_N}(x) = \sum_{k=0}^{\infty}\zeta'(k,N)\frac{d^{4k}}{dx^{4k}}F^{-1}\left\{e^{-0.25N\omega^2}\right\}$$
$$= \sum_{k=0}^{\infty}\zeta'(k,N)\frac{d^{4k}}{dx^{4k}}\left(\frac{1}{\sqrt{\pi N}}e^{-x^2/N}\right). \quad (25)$$

This pdf for (5) can be expressed even more plainly as

$$f_{V_N}(x) \;=\; \frac{1}{\sqrt{\pi N}}\sum_{k=0}^{\infty}\zeta'(k,N)\,h^{(4k)}(x) \quad (26)$$

where $h(x) \;:=\; e^{-x^2/N}$.

Interestingly, the first term of the series (26) as $\frac{e^{-x^2/N}}{\sqrt{N\pi}}$ corresponds to Gaussian distribution with a variance of $0.5N$, and hence, we can deduce that

$$\sum_{k=1}^{\infty}\zeta'(k,N)\,h^{(4k)}(x) \to 0. \quad (27)$$

Note that this deduction was also verified by numerical means via a computer simulation from ζ_k values obtained using (23). Finally, the pdf does simplify to Gaussian distribution

$$f_{V_N}(x) \;=\; \frac{e^{-x^2/N}}{\sqrt{N\pi}}. \quad (28)$$

The pdf $\tilde{f} = f_{V_N^2}$ for $(\sum_{n=1}^{N} y_n x_n)^2$ can be simply accessed by using the formula [12]

$$\tilde{f}(x) = \begin{cases}\dfrac{f(\sqrt{x})}{\sqrt{x}}, & x \geq 0\\ 0, & \text{elsewhere.}\end{cases} \quad (29)$$

Then, the probability *distribution* function $\tilde{F}$ for the random variable V_N^2 is computed through the integration of its pdf

$$\tilde{F}(x) = \int_{-\infty}^{x}\tilde{f}(t)dt = \int_0^x \frac{f(\sqrt{t})}{\sqrt{t}}dt = \left[2F(\sqrt{t})\right]_o^x$$
$$\tilde{F}(x) = 2F(\sqrt{x}) - 1. \quad (30)$$

The probability distribution function *F* can be expressed in terms of error function via an integration of (28)

$$F(x) = \frac{1}{\sqrt{N\pi}}\int_{-\infty}^{x}e^{-\frac{x^2}{N}}dx = 0.5 + \frac{1}{\sqrt{N\pi}}\int_0^x e^{-\frac{x^2}{N}}dx$$
$$= 0.5 + 0.5\mathrm{erf}\left(\frac{x}{\sqrt{N}}\right). \quad (31)$$

Then, by combining (30) and (31), we conclude that

$$\tilde{F}(x) = \mathrm{erf}\left(\sqrt{\frac{x}{N}}\right). \quad (32)$$

B. Statistical Test for Determining Significance of PAC Estimates

Our derivations lead to the simple and compact formula of (32). This formula depends solely on the length of the data sequence *N*. Hence, we can compute the necessary coupling

statistics x for a confidence level of p

$$r = \mathrm{erf}\left(\sqrt{\frac{x_{\lim}}{N}}\right) \Rightarrow x_{\lim} = N \times \left[\mathrm{erf}^{-1}(r)\right]^2 \tag{33}$$

where $r = 1-p$.

The following steps can then be used to compute the confidence level for any frequency pair.

1) Normalize the amplitude vector, i.e., divide the amplitude vector a_H by its standard deviation and subtract the mean to conform to the assumption in the previous section. This normalized vector is denoted by $\tilde{a}_H$.
2) Compute $s = |\sum_{n=1}^{N} \tilde{a}_H(n) e^{i\varphi_L(n)}|^2$ statistics for each frequency pair.
3) Only if $s > 2x_{\lim}$, then accept the corresponding coupling estimate to be reliable. Otherwise, nullify it.

C. Normalized Direct PAC Estimate (ndPAC)

The amplitude time series is normalized (mean removed and variance made unity) when computing the PAC estimate

$$\hat{\rho}_{ND} := \frac{1}{N}\left|\sum_{n=1}^{N} \tilde{a}_H(n) e^{i\varphi_L(n)}\right| \tag{34}$$

for each frequency pair. Normalization helps eliminate distortions in PAC estimate due to dc components in data. Note that the suggested method of ndPAC includes a statistical thresholding procedure described in Section II-B.

III. Experiments

A. Numerical Validation

In order to confirm the derivations given in Section II-A, we produced random Gaussian sequences of s_1 and s_2 with $a(n) \sim N(0,1)$ representing mean removed "amplitude vectors" and uniformly distributed random sequences $b(n) \sim U(-\pi, \pi)$ representing 'phase vectors' for various data lengths of $N = 100$, 500, 1000, 5000, 10000, 100000. This production was repeated 1000 times and these values were computed for each run and for each data length

$$s_1 = \left(\sum_{n=1}^{N} a(n)\cos(b(n))\right)^2, \quad s_2 = \left(\sum_{n=1}^{N} a(n)\sin(b(n))\right)^2. \tag{35}$$

Using MATLAB histogram function *hist*, we composed "empirical cumulative distribution functions" for each of these values. When they were compared to the derived "analytical cumulative distribution function" given by (32), it was observed that these were indistinguishable for sequences of s_1 and s_2 [see Fig. 1(a)].

In order to quantify the similarity observed in Fig. 1(a), we applied Kolmogrov–Smirnov test [19] to determine whether the produced artificial sequences really come from the derived probability distribution. The null hypothesis as "the values come from the proposed distribution" was tested at the significance level of $p = 0.05$. The proposed distribution was calculated from (32) by evaluating it from $x = 0$ up to the maximum value of s_1 and s_2 being varied by the steps of unity. For each data length N, we repeated producing all data and realizing the test 100 times. The null hypothesis acceptance rates for each data length are exhibited in Fig. 1(b). More than 90% of the simulated random sequences significantly belonged to the derived probability distribution [see Fig. 1(b)] for data length over 100. When data were short as $N = 100$, the acceptance rates were slightly under 90%.

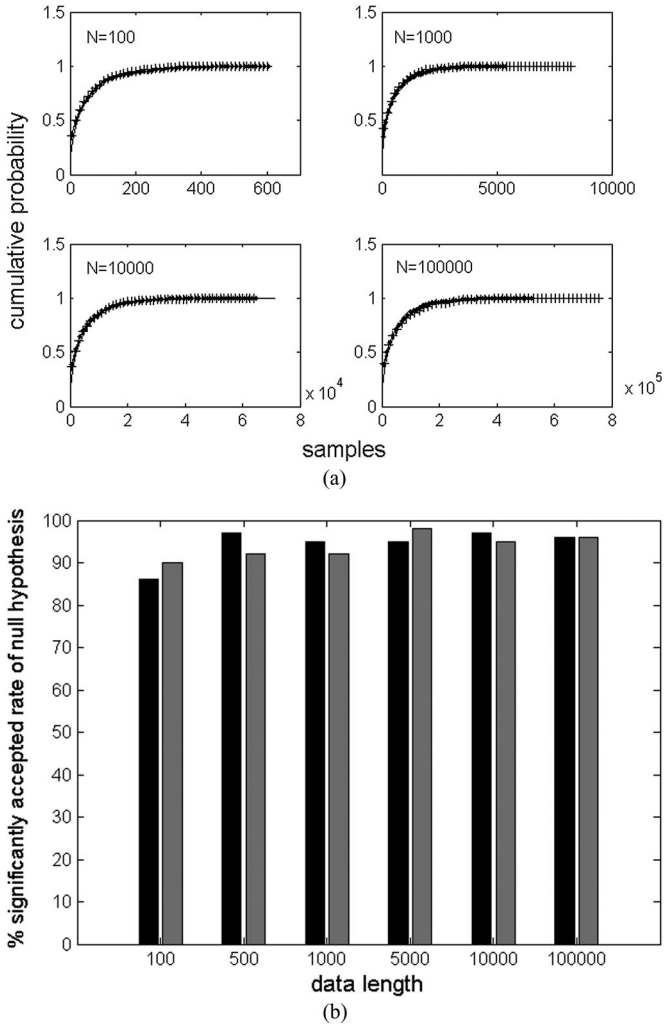

Fig. 1 Numerical validation of confidence level derivation. (a) Derived and hypothesized probability distribution (solid -) for dPAC estimate is indistinguishable from "empirical probability distributions" (plus +, dot .). The mean of "empirical probability distributions" is plotted over 100 realizations. Hypothesized and empirical probability distributions overlap. (b) Kolmogrov–Smirnov test showed that the simulated sequences (35) belong to the hypothesized distribution (32) for over 90%. Black and gray bars refer to null hypothesis acceptance rates for the sequences s_1 and s_2, respectively. Production of data and application of statistical test was realized 100 times.

B. Simulations

In order to evaulate ndPAC, data containing PAC were simulated by adding a Hanning-tapered smooth high-frequency activity (75 Hz) coinciding with a specific phase of a sinusoid (10 Hz) for each cycle [20]. High-frequency activity coupling with the phase of the sinusoid was generated by bandpass filtering random white noise at 70–80 Hz. The sampling frequency was

1 kHz. PAC estimation was realized by two-way least-squares finite impulse response filtered signals using *eegfilt* routine from EEGLAB toolbox [21]. Filter order was three cycles of the corresponding frequency band. The first and last second of data were dropped to avoid any possible edge effects caused by filtering [21], [22]. The bandwidth for low frequencies was 2 Hz, while it was chosen as 10 Hz for high frequencies. Amplitudes and phases from bandfiltered signals were extracted using Hilbert transform. We applied modulation index with statistics (MIS) [23]

$$\hat{\rho}_{\mathrm{MI}} := \left| \sum_{n=1}^{N} a_H(n) e^{i\varphi_L(n)} \right| \tag{36}$$

that includes an additional permutation-based test for statistical thresholding and dPAC [5] (including no statistical test) in order to compare with the proposed methodology of ndPAC provided in detail in Section II. The number of surrogate data for MIS obtained by a shifting operation [23] on amplitudes was taken as 200. Note that the MIS measure includes an extra normalization over (36) by a subtraction from mean of surrogate data modulation index (MI) estimates and a division by their standard deviation as described in [23]. Confidence level was taken as $p = 0.01$ for both ndPAC and MIS methods. All estimates below the confidence level were nullified for both methods.

High-frequency oscillations typically belong to local networks and are confined to small neuronal space, while low-frequency oscillations generally represent larger neuronal networks [4]. Resulting electromagnetic brain oscillations tend to have *1/f* like power spectra, which refers to a linear decrease of power with the increase of freqency on a natural logarithmic scale [24]. Accordingly, synthetic *1/f* noise was added to the synthesized signal in order to test the robustness of the methods to background activity. The energy of *1/f* noise was kept at the same amount with the signal. Synthetic *1/f* noise was produced using "spectral synthesis method" [25]. This method relies on constructing power-law relationship for the signal in the frequency domain and taking the inverse Fourier transform to reconstruct it in the time domain. We took the power exponent of *1/f* noise as $\beta = 1.8$ in our experiments. The generated signal with this particular exponent corresponds to fractional Brownian motion sequences with the Hurst parameter of 0.4 [25], [26]. We further added random Gaussian white noise at different levels of signal to noise ratio (SNR) from -10 to 10 dB. Simulations were repeated 100 times for each estimator and specific condition.

Sensivity and specificity measures were defined to quantify the performance of methods. We accepted estimates at the range *R* of 7–13 Hz for phase frequency and 65–85 Hz for amplitude frequency as the grids of true identification (see Fig. 2). All estimates at the grids outside this range as R' were accepted as false.

All grids of PAC estimation are denoted by $T = R \cup R'$. Accordingly, specificity performance was mean of all estimates at *R* divided by mean of estimates at *T*. Sensitivity performance measure was "binary": if maximum coupling strength belonged to *R*, it was 1; otherwise, the sensitivity was accepted as 0. Note that the sensitivity definition is only valid for the specific simulation design here as we know *a priori* that there is no coupling outside *R*. Simulations and PAC estimation methods were all implemented in MATLAB (Mathworks Inc., Natick, MA). The MATLAB routines are freely available upon request from the author.

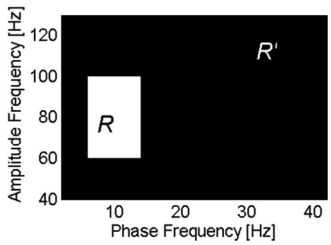

Fig. 2 Sensitivity measure for simulations was accepted 1 when the maximum PAC belonged to *R* and it was 0 if maximum PAC was elsewhere. The specificity measure for simulations was computed as the mean PAC strength in the region *R* divided by mean of all PAC estimates at $T = R \cup R'$.

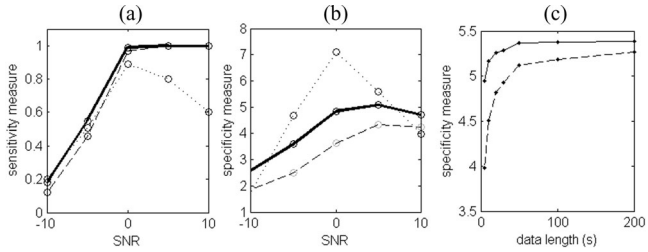

Fig. 3 (a) Sensitivity and (b) specificity performances of ndPAC (bold solid line) compared with dPAC (dashed line) and MIS (dotted line) methods with respect to noise level and (c) ndPAC (solid line) and dPAC (dashed line) specificity performances with respect to data length. Note that MIS specificity performance with respect to data length was not included due to its irregular behavior. ndPAC estimates show consistent increased specificity and sensitivity performances with increased SNR and data length, unlike MIS. All measures were obtained by averaging over 100 repetitions.

We tested the behavior of "ndPAC methodology" with respect to noise strength and data length. ndPAC was more likely to yield accurate PAC estimates hitting on the target when compared with dPAC [see Fig. 3(a)]. This result implies that the "normalization" procedure given in Section II-C increases sensitivity of the estimator.

Moreover, some extra spurious PAC estimates are eradicated due to confidence bound thresholding inherent to the ndPAC method. This also gives better specificity for ndPAC than PAC method [see Fig. 3(b)].

As the data length increased, so does the specificity of "normalized PAC method" [see Fig. 3(c)]. The plateau for specificity is reached at around data length of 50 s. This result implies that the bias of normalized PAC estimate declines as the data get longer. The specificity did not regularly change with respect to data length for MIS. Interestingly, MIS shows erratic behavior also with respect to Gaussian noise level of the signal for both sensitivity and specificity [see Fig. 3(a) and (b)]. When there is too much noise (*1/f* noise + Gaussian noise at SNR $= -5$ dB), MIS might not identify the correct PAC (see Fig. 4, top) at all. Even when the signal is not contaminated with strong white Gaussian noise (SNR $= 10$ dB) but only with *1/f* noise, it might determine the significance level inaccurately. Since statistical

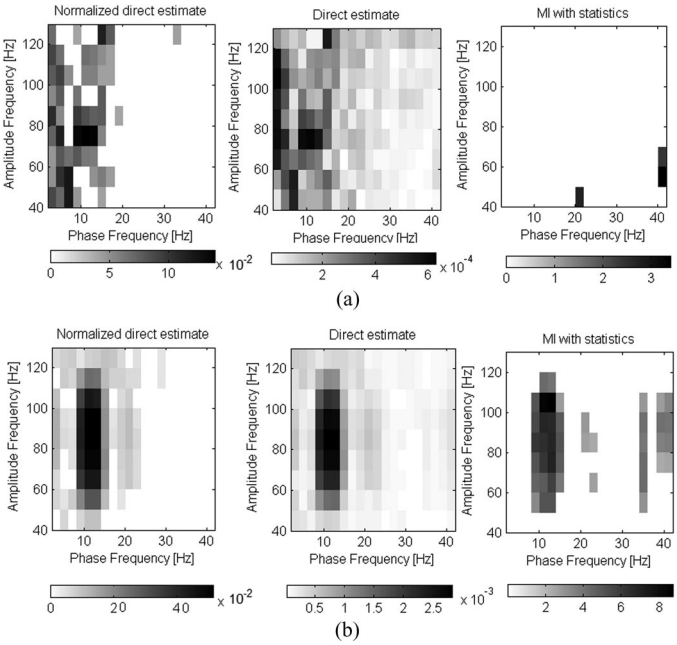

Fig. 4 Coupling portraits of ndPAC (left), dPAC (middle), and MIS (right) of simulated data for (a) SNR $= -5$ dB and (b) SNR $= 10$ dB. ndPAC estimation might yield more reliable estimates when compared with statistically normalized MI and dPAC. When SNR is low, (a) MIS might miss the correct PAC estimate (phase frequency: 10 Hz; amplitude frequency 70–80 Hz) and when SNR is high, (b) it might incorrectly identify the maximum PAC. ndPAC is expected to yield higher specificity performance when compared with dPAC due to the "confidence level thresholding" applied for the former (compare left and middle panels for both SNR levels).

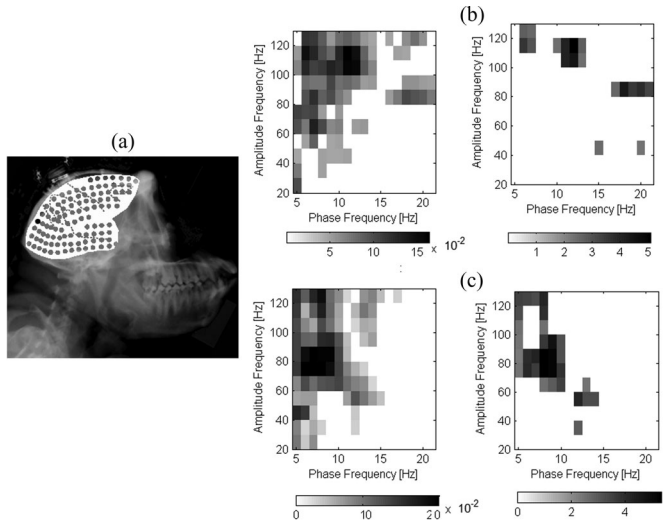

Fig. 5 Coupling portraits obtained from (a) a monkey ECoG posterior channel (marked with a filled circle) for two different visual stimulus conditions of (b) and (c). ndPAC revealed couplings [(b), left panel] between alpha (10–12 Hz) and high gamma (100–110 Hz) for grating pattern angle of 180°, which [(c), left panel] switched between theta (5–10 Hz) and gamma (70–90 Hz) when the angle was 360°. These couplings could be verified with MIS [(b) and (c), right panels].

normalization includes a subtraction by the significance level determined from surrogate data, any chance incidence due to permutation test leads to false PAC estimates (see Fig. 4, bottom). Penny *et al.* [22] did not include MIS in their study, since they reported "it does not have 'good' statistical properties." The inconsistency with statistical behavior might stem from chance-based determination of confidence level from a limited number of surrogate data (typically about 200).

C. Real Data

The methods were applied on monkey electrocorticogram (ECoG) data obtained during a visual task. Data were recorded by Laboratory for Adaptive Intelligence, RIKEN Brain Science Institute, Tokyo, Japan, and was made open to public use [27]. The monkey was reported to be sitting with his head and arms fixed facing a monitor. A grating pattern was moved in several directions while data were acquired with an ECoG array containing 128 channels at the sampling frequency of 1 kHz. For more details on thedata collection procedure, the reader is referred to http://neurotycho.org. Signals were rereferenced to a common average and a notch filter at 50 Hz was applied to eliminate the power line noise. Note that ECoG signals are known to contain "high" SNR, as they represent direct brain activity with a high spatial resolution due to their invasive nature.

We chose one of the channels in the occipital region [see Fig. 5(a)] and evaluated the status of PAC parameters in this channel depending on the grating pattern angle of 180° (condition 1) and 360° (condition 2). Using the stimulus event markings, we classified data corresponding to conditions 1 and 2. The data length for each condition was 40 s. ndPAC identified the maximum clustered coupling between alpha (10–12 Hz) and high gamma (100–110 Hz) for condition 1 [see Fig. 5(b), left panel], while for condition 2, the maximum coupling switched between theta (5–10 Hz and gamma (70–90 Hz) [see Fig. 5(c), left panel]. Identical coupling spots were also detected when MIS was used as the estimator [see Fig. 5(b) and (c), right panels].

IV. Discussion

Neurophysiological signals are assumed to contain various oscillatory components that do not necessarily associate with any coupling relation. Therefore, an ideal PAC estimation should not only capture the PAC relations in the signals but it should also be able to reject false estimates arising from distortions of noncoupled oscillation powers, i.e., it should have high specificity.

This study introduced a methodology called ndPAC for statistically *reliable* estimation of PAC strength. This was achieved via the derivation of an analytical formula for PAC strength confidence. The determined confidence limit could eradicate a certain amount of noncoupled frequency pairs in PAC portraits as illustrated both by simulations and real data. Henceforth, it was possible to increase the *specificity* of PAC estimation via thresholding the PAC estimates by the determined confidence bounds without additional computational expense. Moreover, the *sensitivity* for dPAC estimations was increased with normalization of amplitude time series (see Fig. 3). Normalization also ensured robustness to possible dc-based distortions in the estimates. Simulation results further indicated that ndPAC was

statistically consistent unlike MIS and gave estimates whose specificity increased with the data length.

Another desired property for a PAC estimator would be the *rapid* assessment of the confidence for each phase-amplitude frequency pair. The most popular way to assess significance in neuroscience community hitherto has been permutation-based test supplemented also to "MI" [23]. In this approach, the amplitude time series are shuffled on the orders of 100 in order to produce surrogate data. Then, PAC estimation is carried out for each frequency pair and for each surrogate data. Finally, a statistically reliable PAC limit is obtained by fitting a Gaussian curve to the computed surrogate data PAC estimates. If the PAC estimate for real data is greater than this limit, one could accept it as statistically reliable estimate. A similar permutation-based test with surrogate data was utilized for many diverse PAC estimation methodologies such as cross-frequency coherence [28], phase-locking value-based- [22], amplitude power spectrum-based- [29] and entropy-based [30] methods.

One should keep in mind that PAC estimation typically involves many bandpass filtering and Hilbert transform operations. Accordingly, permutation statistics suffers from computational burden because of repetition of the estimate 100 times for each surrogate data. This slows down the execution dramatically in a standard run when compared with dPAC estimation. Therefore, considering the established potential importance of PAC phenomenon in neural recordings, a quicker way of obtaining statistical reliability for PAC estimates would be beneficial. For instance, capturing transient changes in PAC parameters requires fast and reliable computations. A fast reliable estimation would also be indispensable while searching PAC in overwhelmingly long neurophysiological data sequences.

Our derivation of PAC confidence limit for ndPAC can be considered analogous to analytic "coherence" confidence limit formulation where the coherence significance is computed with a simple expression depending on data length, window length, and confidence level [31], [32]. It should be noted that many studies preferred this formula to determine the significance of the estimated coherence (e.g., [33]–[35]). The approximate coherence confidence formula was derived under the assumption of white Gaussian probability distribution for the time series for which the coherence is computed [31], [32]. Similarly, our study assumes reasonable probability distributions (Gaussian pdf for time series and uniform pdf for phase) for the sequences in order to obtain a simple useful formula for approximate significance limits of dPAC estimates. It provides the necessary tool for rapid computation of confidence limits without paying any additional computational cost to the PAC estimation itself. Similar to the formula suggested for coherence [32], the confidence limit for PAC is computed with a plain formula given in (33) which depends solely on the data length and the confidence level. Determining a lower limit for the significance of PAC enabled an increase in the specificity of the estimator without additional computational burden (see Figs. 3 and 4).

It might be argued that uniform distribution for phase values might be a rather strong assumption for some cases. This is especially true for very short time windows where phase might be reset by some impulsive event such as an external stimulus. However, ndPAC as a member of MI estimator family is not suitable for short time data in general. This can be sensed by the incremental performance of ndPAC as the data get longer [see Fig. 3(c)]. A thorough experimental PAC study [37] also demonstrates that data should be long enough (their suggestion for length limit is >30 s) to compute cross-frequency coupling reliably. It is reasonable to consider that ongoing long enough EEG data tend to have uniform phase distribution in general. For example, Breakspear and Terry [38] took randomly chosen epochs from EEG segments and indicated that phase is uniformly distributed. Another study by Busch *et al.* [39] also showed that phase values of EEG data across all trials were uniform.

In any case, when there is doubt about strong deviations from uniformity in data phase, the practitioner might wish to use statistical tests while applying ndPAC to her data. Rayleigh test [40] is such a test particularly suitable to check whether phase values deviate from uniformity. Note that when Rayleigh test was applied to ECoG data used in this study, we could verify that alpha and theta phases for both conditions do indeed fit into uniform distribution.

We applied the proposed methodology to monkey ECoG data in order to demonstrate its behavior under realistic scenarios. Low-frequency phase coupled to gamma band power as part of a visual attention system was first reported in a monkey study [36]. PAC between theta/alpha phase values and high gamma band amplitude values was also shown to have extensive presence during visual tasks [8]. Our results indicated that the ndPAC method could reveal significant couplings between theta/alpha and high gamma activity from an electrode inserted around the occipital regions of a monkey. Moreover, the coupling phase frequency modulated between theta and alpha depending on the angle of the visual grating pattern (see Fig. 5).

We conclude by underlying the significance of the chosen PAC estimation methodology while evaluating the data under hand. Considering the huge datasets dealt within neuroscience, ndPAC is a promising alternative offering rapid and reliable PAC estimations. This capability of ndPAC becomes especially crucial while cracking the couplings embedded in the brain code occurring between different numerous combinations of neuronal regions.

ACKNOWLEDGMENT

The author would like to thank E. K. Özay, Dr. H. Hacıhabiboğlu, and Dr. Ö. Karabacak for thoughtful discussions. The author would also like to thank the Department of Electronics and Communications Engineering, Istanbul Technical University, and in particular Dr. T. Akgül for allowance to use facilities.

REFERENCES

[1] M. X. Cohen, "It's about time," *Frontiers Human Neurosci.*, vol. 5, 16 pp., Jan. 2011, doi: 10.3389/fnhum.2011.00002.

[2] P. G. Schyns, G. Thut, and J. Gross, "Cracking the code of oscillatory activity," *PLoS Biol.*, vol. 9, no. 5, e1001064, 8 pp., May 2011, doi:10.1371/journal.pbio.1001064.

[3] O. Jensen and L. L. Colgin, "Cross-frequency coupling between neuronal oscillations," *Trends Cognitive Sci.*, vol. 11, no. 7, pp. 267–269, Jul. 2007.
[4] R. T. Canolty and R. T. Knight, "The functional role of cross-frequency coupling," *Trends Cognitive Sci.*, vol. 14, no. 11, pp. 506–515, Nov. 2010.
[5] T. E. Özkurt and A. Schnitzler, "A critical note on the definition of phase-amplitude cross-frequency coupling," *J. Neurosci. Methods*, vol. 201, pp. 438–443, Aug. 2011.
[6] B. Händel and T. Haarmeier, "Cross-frequency coupling of brain oscillations indicates the success in visual motion discrimination," *NeuroImage*, vol. 45, no. 3, pp. 1040–1046, Apr. 2009.
[7] M. X. Cohen, N. Axmacher, D. Lenartz, C. E. Elger, V. Sturm, and T. E. Schlaepfer, "Good vibrations: Cross-frequency coupling in the human nucleus accumbens during reward processing," *J. Cognit. Neurosci.*, vol. 21, no. 5, pp. 875–889, May 2009.
[8] B. Voytek, R. T. Canolty, A. Shestyuk, N. E. Crone, J. Parvizi, and R. T. Knight, "Shifts in gamma phase-amplitude coupling frequency from theta to alpha over posterior cortex during visual tasks," *Frontiers Human Neurosci.*, vol. 4, 9 pp., Jan. 2010, doi: 10.3389/fnhum.2010.00191.
[9] N. Axmacher, M. M. Henseler, O. Jensen, I. Weinreich, C. E. Elger, and J. Fell, "Cross-frequency coupling supports multi-item working memory in the human hippocampus," *Proc. Natl. Acad. Sci. U.S.A.*, vol. 107, no. 7, pp. 3228–3233, Feb. 2010.
[10] J. López-Azcárate, M. Tainta, M. C. Rodriguez-Oraz, M. Valencia, R. González, J. Guridi, J. Iriarte, J. A. Obeso, J. Artieda, and M. Alegre, "Coupling between beta and high-frequency activity in the human subthalamic nucleus may be a pathophysiological mechanism in Parkinson's disease," *J. Neurosci.*, vol. 30, no. 19, pp. 6667–6677, May 2010.
[11] T. E. Özkurt, M. Butz, M. Homburger, S. Elben, J. Vesper, L. Wojtecki, and A. Schnitzler, "High frequency oscillations in the subthalamic nucleus: A neurophysiological marker of the motor state in Parkinson's disease," *Exp. Neurol.*, vol. 229, no. 2, pp. 324–331, Jun. 2011.
[12] H. Stark and J. W. Woods, *Probability and Random Processes With Applications to Signal Processing*. Englewood Cliffs, NJ: Prentice-Hall, 2002.
[13] V. K. Rohatgi, *An Introduction to Probability and Statistics*. New York: Wiley, 1976.
[14] G. B. Thomas and R. L. Finney, *Calculus and Analytic Geometry*. Reading, MA: Addison-Wesley, 1996.
[15] I. S. Gradshteyn and I. M. Ryzhik, *Table of İntegrals, Series and Products*. New York: Academic, 1980.
[16] G. E. Andrews, R. Askey, and R. Roy, *Special Functions (Encyclopedia of Mathematics and its Applications)*. Cambridge, U.K.: Cambridge Univ. Press, 1999.
[17] M. Abramowitz and I. A. Stegun, *Handbook of Mathematical Functions With Formulas, Graphs, and Mathematical Tables*. New York: Dover, 1965.
[18] Á. Baricz, "Powers of modified Bessel functions of the first kind," *Appl. Math. Lett.*, vol. 23, no. 6, pp. 722–724, Jun. 2010.
[19] F. J. Massey, "The Kolmogrov–Smirnov test for goodness of fit," *J. Amer. Stat. Assoc.*, vol. 46, no. 253, pp. 68–78, 1951.
[20] M. Kramer, A. B. L. Tort, and N. J. Kopell, "Sharp edge artifacts and spurious coupling in EEG frequency comodulation measures," *J. Neurosci. Methods*, vol. 170, no. 2, pp. 352–357, May. 2008.
[21] A. Delorme and S. Makeig, "EEGLAB: An open source toolbox for analysis of single-trial EEG dynamics including independent component analysis," *J. Neurosci. Methods*, vol. 134, no. 1, pp. 9–21, 2004.
[22] W. D. Penny, E. Duzel, K. J. Miller, and J. G. Ojemann, "Testing for nested oscillation," *J. Neurosci. Methods*, vol. 174, no. 1, pp. 50–61, Sep. 2008.
[23] R. T. Canolty, E. Edwards, S. S. Dalal, M. Soltani, S. S. Nagarajan, H. E. Kirsch, M. S. Berger, N. M. Barbaro, and R. T. Knight, "High gamma power is phase-locked to theta oscillations in human neocortex," *Science*, vol. 313, no. 5793, pp. 1626–1628, Sep. 2006.
[24] G. Buzsáki and A. Draguhn, "Neuronal oscillations in cortical networks," *Science*, vol. 304, no. 5679, pp. 1926–1929, 2004.
[25] D. G. Manolakis, V. K. Ingle, and S. M. Kogon, *Statistical and Adaptive Signal Processing*. New York: McGraw-Hill, 2000.
[26] B. B. Mandelbrot and J. W. Van Ness, "Fractional Brownian motions, fractional noise and applications," *SIAM Rev.*, vol. 10, no. 4, pp. 422–437, 1968.
[27] Y. Nagasaka, K. Shimoda, and N. Fujii, "Multidimensional recording (MDR) and data sharing: An ecological open research and educational platform for neuroscience," *PLoS One*, vol. 6, no. 7, e22561, 17 pp., Jul. 2011, doi:10.1371/journal.pone.0022561.
[28] D. Osipova, D. Hermes, and O. Jensen, "Gamma power is phase-locked to posterior alpha activity," *PloS One*, vol. 3, no. 12, e3990, 7 pp., Jan. 2008, doi:10.1371/journal.pone.0003990.
[29] M. X. Cohen, "Assessing transient cross-frequency coupling in EEG data," *J. Neurosci. Methods*, vol. 168, no. 2, pp. 494–499, Mar. 2008.
[30] A. B. L. Tort, M. A. Kramer, C. Thorn, D. J. Gibson, Y. Kubota, A. M. Graybiel, and N. J. Kopell, "Dynamic cross-frequency couplings of local field potential oscillations in rat striatum and hippocampus during performance of a T-maze task," *Proc. Natl. Acad. Sci. U.S.A.*, vol. 105, no. 51, pp. 20517–20522, Dec. 2008.
[31] V. Benignus, "Estimation of the coherence spectrum and its confidence interval using the fast Fourier transform," *IEEE Trans. Audio Electroacoust.*, vol. 17, no. 2, pp. 145–150, Jun. 1969.
[32] D. M. Halliday, J. R. Rosenburg, A. M. Amjad, P. Breeze, B. A. Conway, and S. F. Farmer, "A framework for the analysis of mixed time series/point process data–theory and application to the study of physiological tremor, single motor unit discharges and electromyograms," *Prog. Biophys. Mol. Biol.*, vol. 64, pp. 237–278, 1995.
[33] J. Gross, J. Kujala, M. Hamalainen, L. Timmermann, A. Schnitzler, and R. Salmelin, "Dynamic imaging of coherent sources: Studying neural interactions in the human brain," *Proc. Natl. Acad. Sci. U.S.A.*, vol. 98, no. 2, pp. 694–699, Jan. 2001.
[34] M. Weinberger, N. Mahant, W. D. Hutchison, A. M. Lozano, E. Moro, M. Hodaie, A. E. Lang, and J. O. Dostrovsky, "Beta oscillatory activity in the subthalamic nucleus and its relation to dopaminergic response in Parkinson's disease," *J. Neurophysiol.*, vol. 96, no. 6, pp. 3248–3256, Dec. 2006.
[35] J. Hirschmann, T. E. Özkurt, M. Butz, M. Homburger, S. Elben, C. J. Hartmann, J. Vesper, L. Wojtecki, and A. Schnitzler, "Distinct oscillatory STN-cortical loops revealed by simultaneous MEG and local field potential recordings in patients with Parkinson's disease," *Neuroimage*, vol. 55, no. 3, pp. 1159–1168, Apr. 2011.
[36] P. Lakatos, A. S. Shah, K. H. Knuth, I. Ulbert, G. Karmos, and C. E. Schroeder, "An oscillatory hierarchy controlling neuronal excitability and stimulus processing in the auditory cortex," *J. Neurophysiol.*, vol. 94, pp. 1904–1911, 2005.
[37] A. B. L. Tort, R. Komorowski, H. Eichenbaum, and N. Kopell, "Measuring phase-amplitude coupling between neuronal oscillations of different frequencies," *J. Neurophysiol.*, vol. 104, no. 2, pp. 1195–1210, 2010.
[38] M. Breakspear and J. R. Terry, "Detection and description of non-linear interdependence in normal multichannel human EEG data," *Clin. Neurophysiol.*, vol. 113, pp. 735–753, 2002.
[39] N. A. Busch, J. Dubois, and R. Vanrullen, "The phase of ongoing EEG oscillations predicts visual perception," *Trends Cognitive Sci.*, vol. 29, no. 24, pp. 7869–7876, 2009.
[40] N. I. Fisher, *Statistical Analysis of Circular Data*. Cambridge, U.K.: Cambridge Univ. Press, 1995.

Tolga Esat Özkurt was born in Istanbul, Turkey, in 1980. He received the B.Sc. degree in electronics and communications engineering and the M.Sc. degree in computer science from Istanbul Technical University, Istanbul, in 2002 and 2004, respectively, and the Ph.D. degree in electrical and computer engineering from the University of Pittsburgh, Pittsburgh, PA, in 2009.

During 2009–2011, he was a Postdoctoral Researcher with the Institute for Medical Psychology and Clinical Neuroscience, Heinrich Heine University, Düsseldorf, Germany. In June 2011, he received a personal research grant from the Scientific and Technological Research Council of Turkey to pursue a research project regarding cross-frequency coupling. He is currently an Assistant Professor in the Department of Health Informatics, Informatics Institute, Middle East Technical University, Ankara, Turkey. His current research interests include neuroimaging and biomedical signal processing.